Dielectrowetting Driven Spreading of Droplets

G. McHale,* C. V. Brown, M. I. Newton, G. G. Wells, and N. Sampara

School of Science and Technology, Nottingham Trent University, Clifton Lane, Nottingham NG11 8NS, United Kingdom

(Received 8 August 2011; published 25 October 2011)

The wetting of solid surfaces can be modified by altering the surface free energy balance between the solid, liquid, and vapor phases. Here we show that liquid dielectrophoresis induced by nonuniform electric fields can be used to enhance and control the wetting of dielectric liquids. In the limit of thick droplets, we show theoretically that the cosine of the contact angle follows a simple voltage squared relationship analogous to that found for electrowetting on dielectric. Experimental observations confirm this predicted dielectrowetting behavior and show that the induced wetting is reversible. Our findings provide a noncontact electrical actuation process for meniscus and droplet control.

DOI: 10.1103/PhysRevLett.107.186101 PACS numbers: 68.08.Bc, 68.03.Cd

The wetting of solid surfaces can be modified by changing material or surface properties, such as the surface chemistry or micro- or nanoscale topography [1,2], or by introducing additional energies, such as electrostatic [3]. This is important for a wide range of processes from microfluidics, whereby large surface area to volume ratios lead to the dominant forces being capillary [4], to liquid-based optics, whereby control of the liquid meniscus determines optical properties [5,6]. In recent years, electrowetting on dielectric (EWOD) has been shown to be one of the most versatile and effective methods to actively control the energy balance in the wetting of a solid surface by a droplet [3,7,8]. In this approach, one or more solid electrodes are coated with a hydrophobic dielectric layer and a droplet of a conducting liquid is then used as the other electrode to create a capacitive structure, but with an electrode contact area dependent on the extent to which the dielectric layer is wetted. This effect modifies the energy balance at the three-phase contact line due to charged ions at the solid-liquid interface, resulting in a contact angle which decreases with applied voltage and which can be used to actuate contact line motion.

Electrowetting has found extensive application in microfluidics [9] and digitally controlled droplet-based chemical reactions and biological assays [10,11], liquid paper [12], variable focus liquid lenses [13,14], to control the Cassie-Baxter to Wenzel transition on superhydrophobic surfaces to create reserve batteries [15], and to increase coating speeds [16], to name but a few of its applications. Its functionality has included controlling meniscus curvature, actuating droplet motion, dispensing and mixing liquids and reducing contact angle hysteresis [17]. In general, a liquid subjected to electrostatic fields does not simply show a change in contact angle, but can also experience a strong bulk force [18]. While electrowetting is a versatile method of controlling contact angle, it uses uniform electric fields and requires a conducting liquid in physical contact with an electrode and when operated with a droplet in air often has a high degree of contact angle hysteresis. In this Letter, we show that nonuniform electric fields can be used with dielectric liquids and noncontacting electrodes to achieve analogous control of contact angle over a wide range of contact angles and with low degrees of contact angle hysteresis.

The forces on the two charges of a dipole created by polarizing a region of material in a uniform electric field balance each other, but when this field is nonuniform, one is larger than the other and an overall force occurs. In a dielectric liquid a nonuniform field therefore causes a bulk force and liquid motion [19]. The use of liquid dielectrophoresis on a circular electrode geometry to create a variable focus lens [20] and a microlens array [21] has been reported, but the theoretical relationship to contact angle and wetting has not been elucidated. To understand how liquid dielectrophoresis might be understood within the context of the wider principles of wetting and control of the contact angle of a droplet, we first consider a uniform layer of a dielectric liquid of depth h on a solid surface with an electric potential that decays with depth of penetration into the liquid, i.e., $V(z) = V_0 \exp(-2z/\delta)$, where δ is a penetration depth. The electrostatic energy per unit contact area, w_E, stored in the liquid is then given by integrating the dielectric energy density, $\frac{1}{2}\varepsilon_o\varepsilon_l \underline{E}\cdot\underline{E}$, where ε_l is the dielectric constant of the liquid and $\underline{E} = -\underline{\nabla}V$ is the electric field, over the volume of the liquid in this area,

$$w_E = -\frac{\varepsilon_o\varepsilon_l V_0^2}{2\delta}[e^{-4h/\delta} - 1]. \quad (1)$$

In the limit of a liquid layer which is much thicker than the penetration depth of the electric potential the energy per unit contact area of the liquid is $w_E = \varepsilon_o\varepsilon_l V_0^2/2\delta$. Thus, while liquid dielectrophoresis is, in principle, a bulk force, under these conditions it is the change in contact area that causes a change in the net dielectrophoretic force acting upon the liquid. In essence, the penetration depth of the electric field effectively localizes the effective changes in energy to the vicinity of the solid-liquid interface.

For a droplet, the extent of wetting of a solid surface is given by a local minimum in the surface free energy arising from the solid-vapor, solid-liquid, and liquid-vapor interfaces. These are characterized by three interfacial tensions, γ_{SV}, γ_{SL}, and γ_{LV}, representing the surface energies per unit area. The effect of increasing the contact area by a small amount, ΔA, is to replace the solid-vapor interface by a solid-liquid interface and so change the surface free energy by $(\gamma_{SL} - \gamma_{SV})\Delta A$. In addition, the movement of the liquid creates an additional liquid-vapor surface area of $\Delta A \cos\theta$ resulting in a surface free energy increase of $\gamma_{LV}\Delta A \cos\theta$ [22]. In the presence of the nonuniform electric field, and assuming the droplet is sufficiently thick ($h \gg \delta$), there is an additional energy expended of $-\varepsilon_o(\varepsilon_l - 1)V_0^2\Delta A/2\delta$. For the droplet to be in equilibrium the total change in energy must vanish and so the contact angle adopts a value, $\theta_e(V_0)$, given by,

$$\cos\theta_e(V_0) = \cos\theta_e + \frac{\varepsilon_o(\varepsilon_l - 1)V_0^2}{2\gamma_{LV}\delta} \qquad (2)$$

where Young's law has been used to replace the combination of interfacial tensions by $\cos\theta_e = (\gamma_{SV} - \gamma_{SL})/\gamma_{LV}$. Equation (2) is a liquid dielectrophoresis (L-DEP) modified form of Young's law, which we refer to as ''dielectrowetting'' in recognition of the effect of L-DEP upon the contact angle. This equation is similar in form to the electrowetting-on-dielectric modified Young's law, but with the ratio of the substrate permittivity to substrate dielectric thickness (ε_r/d) replaced by the ratio of liquid permittivity minus that of air to penetration depth $(\varepsilon_l - 1)/\delta$. It is therefore predicted that an exponentially decaying electric field penetrating into a dielectric liquid will enhance wetting, reducing the contact angle according to Eq. (2), and so drive a droplet to spread according to magnitude of voltage applied. Formally, Eq. (2) predicts that a transition to complete wetting, $\theta_e(V_T) = 0$, should occur at a sufficiently high critical voltage, V_T. However, as the droplet spreads and tends to a film its upper liquid-vapor interface comes within the range of the penetration depth. This interface may then change shape, thus providing a mechanism, in addition to the displacement of the three-phase contact line, whereby energy may be minimized [6,23].

To test the prediction of dielectrowetting induced spreading and reduction in contact angle, we initially used 1.29 μl volume droplets of 1, 2 propylene glycol deposited onto a 2 μm thick layer of SU-8 coating a set of parallel interdigitated electrodes of width 80 μm and gap of 80 μm fabricated on glass substrates (Fig. 1). To achieve a high ($\sim 90°$) initial contact angle the SU-8 was treated with hydrophobizing fluorocarbon solution. On applying a 10 kHz sinusoidal voltage of peak amplitude, V, rising from 0 V to 312 V the droplets of liquid increasingly spread along the direction of the electrodes with little or no spreading across the electrodes (Fig. 2). For an

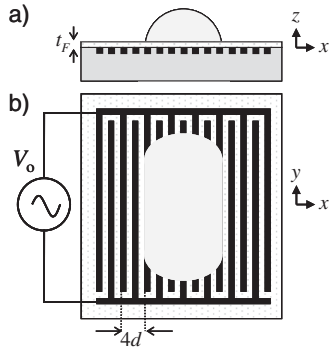

FIG. 1. Schematic of experimental configuration with interdigitated electrode structure with uniform gaps and widths (coated with a thin dielectric layer) generating an exponentially decaying electric field in the vertical direction. Droplet profile viewed (a) parallel to the electrodes, and (b) from above.

electrode width and gap between electrodes of, d, the electrical period is $4d$ giving a wave number $k = \pi/2d$. From Poisson's equation, the solution for the potential in a semi-infinite dielectric liquid is of the form $\sim \cos(kx) \times \exp(-kz)$, so that the penetration depth is related to the electrode structure by $\delta = 4d/\pi$. Because of the periodicity of the electrodes and the energy barriers therefore introduced to motion across the electrodes, the liquid is expected to be confined to motion along the electrodes as observed in Fig. 2. Viewed perpendicular to the direction of spreading, the contact angle falls from 96° to 23° as the voltage is increased and then steadily increases back to 84° as the voltage is steadily diminished.

Figure 3 shows the quasistatic contact angle changes with applied voltage. The initial data point before the application of the voltage lies above the trend of the decreasing contact angle and this is due to it being above the receding contact angle for the surface. Similarly, the initial four data points as the voltage is reduced from its maximum lie away from the trend of the increasing contact angle due to the change from a receding contact angle to an

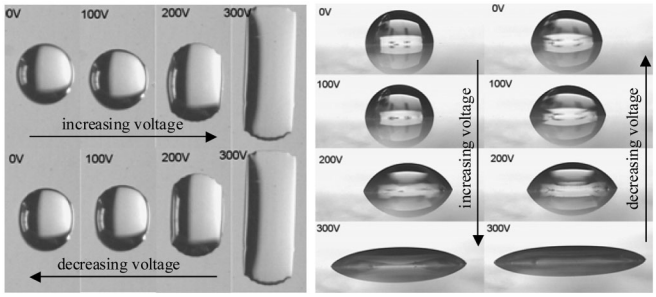

FIG. 2. Images of a 1, 2 propylene glycol droplet on a hydrophobic 2 μm thick SU-8 film on top of parallel planar interdigital electrodes of finger width and gap spacing of 80 μm: Views from above and in side-profile with camera aligned perpendicular to the electrodes as a 10 kHz peak-to-peak sinusoidal voltage is increased from 0 V to 312 V and back to 0 V.

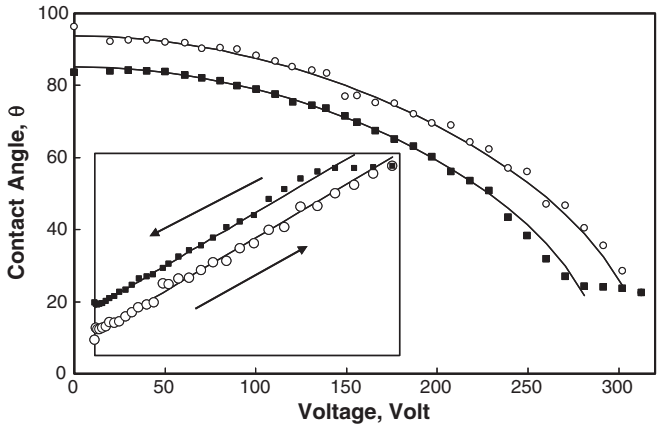

FIG. 3. The contact angle-voltage relationship for the data in Fig. 1 (■ symbols indicate the increasing voltage half-cycle and ○ symbols indicate the decreasing voltage half-cycle). The inset shows the data plotted as cosine contact angle versus voltage squared according to Eq. (2); solid lines are fits to the linear regions using the average slope of the full data set. The hysteresis is caused by the switch from an advancing to a receding contact angle as the voltage changes from increasing to decreasing.

advancing contact angle. In the regions where the contact angle decreases (or increases) steadily with voltage there is a linear dependence of $\cos\theta$ on V^2 as shown in the inset to Fig. 3. The increasing and decreasing voltage half-cycles are offset due to a small $\sim 6°$ contact angle hysteresis. From this we concluded that L-DEP is able to spread droplets and that there is an initial regime, covering a very wide contact angle range ($\sim 70°$), for which the functional form of Eq. (2) applies for this size of electrode structure and droplet volume.

Quantitatively, using the value $\varepsilon_l = 35.0$ for the relative permittivity of the oil and a value of $\gamma_{\mathrm{LV}} = 38\ \mathrm{mN\,m^{-1}}$ for the surface tension so that $(\varepsilon_l - 1)/\gamma_{\mathrm{LV}} = 895\ \mathrm{m\,N^{-1}}$, Eq. (2) predicts the slope of the data in Fig. 3 to be $m_p = 0.39 \times 10^{-4}\ \mathrm{V^{-2}}$. The experimentally observed value of $m_{\mathrm{exp}} = 1.07 \times 10^{-4}\ \mathrm{V^{-2}}$ is of the same order of magnitude. To more accurately compare, we take into account that the SU-8 layer will cause a capacitive division of the voltage so that the effective voltage in the liquid, V_c, is reduced compared to that applied to the interdigitated transducers, V_0. A simple model gives a voltage reduction factor, C, of,

$$C = \frac{(1 + \frac{\Delta\varepsilon}{\varepsilon})e^{-2t_F/\delta}}{1 + (\frac{\Delta\varepsilon}{\varepsilon})e^{-4t_F/\delta}} \qquad (3)$$

where t_F is the thickness of the dielectric layer, $\Delta\varepsilon/\varepsilon = (\varepsilon_{\mathrm{F}} - \varepsilon_{\mathrm{oil}})/(\varepsilon_{\mathrm{F}} + \varepsilon_{\mathrm{oil}})$. For this experiment, using $\varepsilon_{\mathrm{SU8}} = 3$ gives $C = 0.685$ and the theoretical value of the slope is then $C^{-2}m_p = 0.83 \times 10^{-4}\ \mathrm{V^{-2}}$, which is 23% smaller than the experimentally observed value.

We repeated the initial experiments with interdigitated electrodes of reduced widths 20 μm and 40 μm (with gap sizes the same as electrode widths) capped with an SU-8 layer of 0.6 μm, and in each case reversible voltage controlled spreading was observed. The functional form, $\cos\theta \propto V^2$ of Eq. (2) was found to fit the data for both increasing and decreasing voltages, although we did observe a slight systematic reduction of the slope on the reducing voltage half-cycles compared to the increasing voltage half-cycles as electrode size decreased to 20 μm. To compare to the data for the 80 μm width electrodes, Fig. 4(a) shows the decreasing voltage half-cycle for $\cos\theta$ plotted against the ratio of effective voltage V_c^2 to the mechanical pitch $p = 2d$ for the data in Fig. 3 with the data for the two other electrode sizes overlaid. In these cases, the reduction factors C from Eq. (3) which have been used are 0.613, 0.760, and 0.655 for the 20 μm, 40 μm, and 80 μm electrode widths, respectively, where a value $(\varepsilon_l - 1)/\gamma_{\mathrm{LV}} = 1057\ \mathrm{m\,N^{-1}}$ for propylene glycol

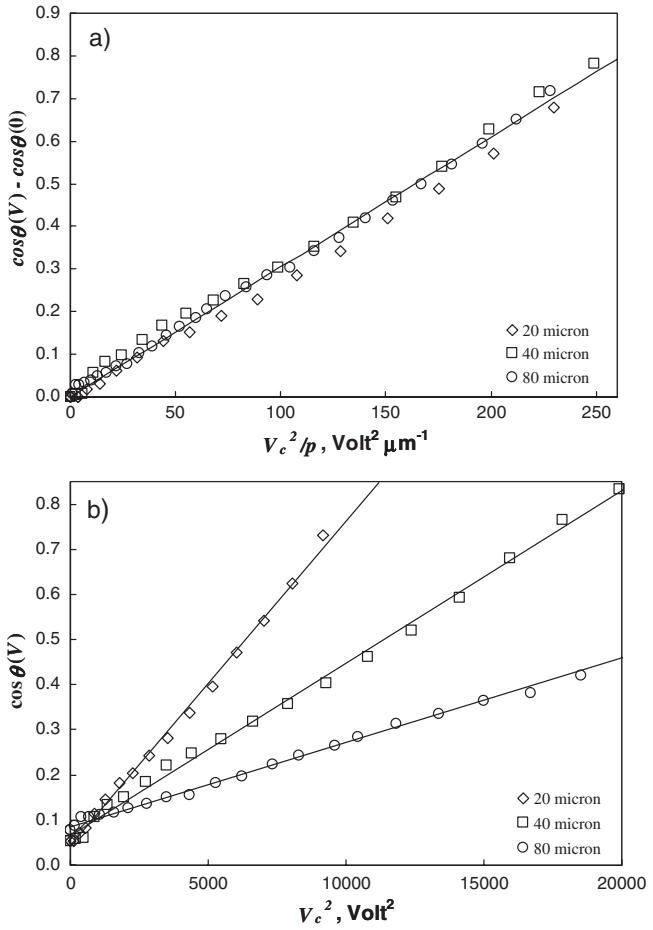

FIG. 4. (a) Data for three electrode pitches (20, 40, and 80 μm) plotted as a function of the effective voltage normalized by electrode mechanical pitch. The effective voltage takes into account the capacitive division caused by the solid dielectric layer on the interdigitated electrodes. (b) Data presented showing the effect of reducing the electric potential penetration depth into the liquid caused by changing the electrode mechanical pitch.

has been used to match the data in Fig. 3. Figure 4(b) shows $\cos\theta$ plotted against the effective voltage V_c^2 for the three electrode pitches; the solid lines are the individual lines of best fit. These data illustrate control of the strength of dielectrowetting by selection of the electrode pitch and, hence, scaling the penetration depth of the electric potential.

In this work, we have focused on droplets which have a thickness greater than the penetration depth set by the nonuniform electric field generated by an interdigitated electrode structure. At these droplet thickness to penetration depth ratios there is little possibility of the liquid-vapor interface beyond the penetration depth deforming to minimize the droplet surface free energy. However, as a droplet becomes thinner and more of a thin liquid film this assumption will break down and the liquid-vapor interface will wrinkle to adjust the overall energy balance between dielectrophoresis and surface free energies. For a planar parallel set of interdigital transducers the free surface of the liquid then first takes on a sinusoidal wrinkled appearance followed by a more complex nonsinusoidal wrinkle reflecting the concentration of electric field gradients at the electrode edges [23]. Here, our studies have also focused on nonaqueous liquids lacking free ionic charges and in air, but may also be relevant to reports of contactless EWOD [24]. Furthermore, electric fields can penetrate salt solutions typically used in electrowetting despite their dc electrical conductivity when they are applied with a sufficiently high frequency [25]. It should therefore be possible to control the droplet contact angle for a full range of liquids simply by choosing a suitably high frequency of applied voltage. This also means that two-liquid systems rather than a liquid droplet in air, necessary for applications such as liquid-optics requiring neutral buoyancy, will be possible.

In summary, our approach shows how liquid dielectrophoresis can be used as an effect to reduce the contact angle of a droplet in a voltage controlled manner. This dielectrowetting effect is complementary to electrowetting, is based upon inhomogeneous electrostatic fields, and does not require the liquid to be conducting or to be contacted by the electrodes. Our observations show that provided the droplet has a thickness larger than the penetration depth of the electric potential the cosine of the contact angle has a simple square law dependence on the applied voltage. The ability to control the contact angle by dielectrowetting has significance for processes such as droplet-based microfluidics, lab-on-a-chip systems, liquid-based optics, coating and other processes where enhanced or controlled spreading are desired. Finally, it is possible that dielectrowetting can be combined with superoleophobicity to create control of nonaqueous droplets across the full contact angle range.

The authors acknowledge the financial support of the UK EPSRC.

*To whom correspondence should be addressed.
glen.mchale@ntu.ac.uk

[1] D. Quéré, Annu. Rev. Mater. Res. **38**, 71 (2008).
[2] N. J. Shirtcliffe, G. McHale, S. Atherton, and M. I. Newton, Adv. Colloid Interface Sci. **161**, 124 (2010).
[3] F. Mugele and J. C. Baret, J. Phys. Condens. Matter **17**, R705 (2005).
[4] T. M. Squires and S. R. Quake, Rev. Mod. Phys. **77**, 977 (2005).
[5] J. Heikenfeld, K. Zhou, E. Kreit, B. Raj, S. Yang, B. Sun, A. Milarcik, L. Clapp, and R. Schwartz, Nat. Photon. **3**, 292 (2009).
[6] C. V. Brown, G. G. Wells, M. I. Newton, and G. McHale, Nat. Photon. **3**, 403 (2009).
[7] M. Vallet, B. Berge, and L. Vovelle, Polymer **37**, 2465 (1996).
[8] B. Berge, C.R. Acad. Sci. Ser. Gen., Ser. 2 **317**, 157 (1993).
[9] D. Mark, S. Haeberle, G. Roth, F. von Stetten, and R. Zengerle, Chem. Soc. Rev. **39**, 1153 (2010).
[10] G. Pollack, R. B. Fair, and A. D. Shenderov, Appl. Phys. Lett. **77**, 1725 (2000).
[11] R. B. Fair, Microfluid. Nanofluid. **3**, 245 (2007).
[12] R. A. Hayes and B. J. Feenstra, Nature (London) **425**, 383 (2003).
[13] B. Berge and J. Peseux, Eur. Phys. J. E **3**, 159 (2000).
[14] S. Kuiper and B. H. W. Hendriks, Appl. Phys. Lett. **85**, 1128 (2004).
[15] T. N. Krupenkin, J. A. Taylor, T. M. Schneider, and S. Yang, Langmuir **20**, 3824 (2004).
[16] T. D. Blake, A. Clarke, and E. H. Stattersfield, Langmuir **16**, 2928 (2000).
[17] F. Li and F. Mugele, Appl. Phys. Lett. **92**, 244108 (2008).
[18] T. B. Jones, Langmuir **18**, 4437 (2002).
[19] T. B. Jones, M. Gunji, M. Washizu, and M. J. Feldman, J. Appl. Phys. **89**, 1441 (2001).
[20] C.-C. Cheng, C. A. Chang, and J. A. Yeh, Opt. Express **14**, 4101 (2006).
[21] Y.-C. Wang, Y.-C. Tsai, and W.-P. Shih, Microelectron. Eng. **88**, 2748 (2011).
[22] P. G. de Gennes, Rev. Mod. Phys. **57**, 827 (1985).
[23] C. V. Brown, W. Al-Shabib, G. G. Wells, G. McHale, and M. I. Newton, Appl. Phys. Lett. **97**, 242904 (2010).
[24] A. G. Banpurkar, K. P. Nichols, and F. Mugele, Langmuir **24**, 10 549 (2008).
[25] T. B. Jones and K. L. Wang, Langmuir **20**, 2813 (2004).